Original Article
Morphological study and comprehensive cellular constituents of milky spots in the human omentum

Jiu-Yang Liu[1], Jing-Ping Yuan[2], Xia-Fei Geng[1], Ai-Ping Qu[3], Yan Li[1]

[1]Department of Oncology, Zhongnan Hospital of Wuhan University, Hubei Key Laboratory of Tumor Biological Behaviors and Hubei Cancer Clinical Study Center, Wuhan 430071, Hubei Province, China; [2]Department of Pathology, Renmin Hospital of Wuhan University, Wuhan, Hubei Province, China; [3]School of Computer, Wuhan University, Wuhan 430071, Hubei Province, China

Abstract: Objective: To analyze morphological features of omental milky spots (MS). Method: Hematoxylin-eosin staining and immunohistochemistry technique were used to study the omental MS of gastric cancer (GC) patients and rectal cancer (RC) patients. We focused on morphological features of MS and conducted quantitative analysis on the cells number and cellular constituents. Differences in MS parameters between GC and RC were also analyzed. Results: Various shapes of MS were mainly round, oval, irregular form in the adipose and perivascular annular. The median MS perimeter was 2752 (range 817~7753) computer-based pixels. The median value of immune cells in one MS was 141 (43~650), comprising T lymphocytes (46.1%), B lymphocytes (28.4%), macrophages (12.4%) and other immune cells (13.1%). Relatively high density of vessels in MS could be calculated by microvessel density (MVD) as 4 (0~13). The median value of mesothelial cells loosely arranged in the surface layer was 5 (0~51). There were no significant differences in MS perimeter, MVD, the number of mesothelial cells, total immune cells, T lymphocytes and macrophages between GC and RC (P>0.05), while the number of MS B lymphocytes in RC was significantly higher than that in GC (P<0.001). Conclusion: MS are primary immune tissues in the omentum and structural bases for development and progression of peritoneal dissemination of GC and RC. Analyzing the morphology and cellular constituents could help understanding the mechanism of peritoneal metastasis.

Keywords: Milky spot, omentum, gastric cancer, rectal cancer, peritoneal metastasis

Introduction

Peritoneal carcinomatosis is a kind of regional metastatic disease arising from intraperitoneal tumors including carcinomas of the stomach, colorectum, and ovary [1-3]. After escaping from the primary tumor, cancer cells in the peritoneal fluid gain access into the peritoneum and can potentially infiltrate within a variety of peritoneal tissues. The omentum is the major site for peritoneal metastasis [4] because of more abundant milky spots (MS) than other tissues in the abdominal cavity such as the mesentery and the pelvic floor. Interspersed within the omentum, MS are specific sites consisting of a complex network of capillaries, aggregates of immune cells and loosely arranged mesothelial cells atop them. These unique microenvironment are adaptive for attachment, survival, and growth of peritoneal free cancer cells (PFCC) to facilitate metastatic colonization within the peritoneal cavity. However, precise cellular constituents of MS still need to be further studied.

This study aimed to conduct quantitative analysis on the histological features, cells number, and cellular composition of MS. These data could help gain a clear understanding of MS at the cytological and histological level to study the peritoneal metastasis of gastric cancer (GC) and rectal cancer (RC).

Materials and methods

Preparation for human omentum tissues

The omenta were obtained from three GC patients and three RC patients, and then fixed

Table 1. Primary antibodies used in this study

| Primary antibody	Clone	Source	Dilution	For
Monoclonal Mouse Anti-Human CD68	PG-M1	Dako, Denmark	Ready-to-use	Macrophages
Monoclonal Mouse Anti-Human CD3	F7.2.38			T lymphocytes
Monoclonal Mouse Anti-Human CD20cy	L26			B lymphocytes
Monoclonal Mouse Anti-Human Calretinin	DAK-Calret 1			Mesothelial cells
Polyclonal Goat Anti-Human CD105	P4A4	Santa Cruz, USA	1:500	Vascular endothelial cells
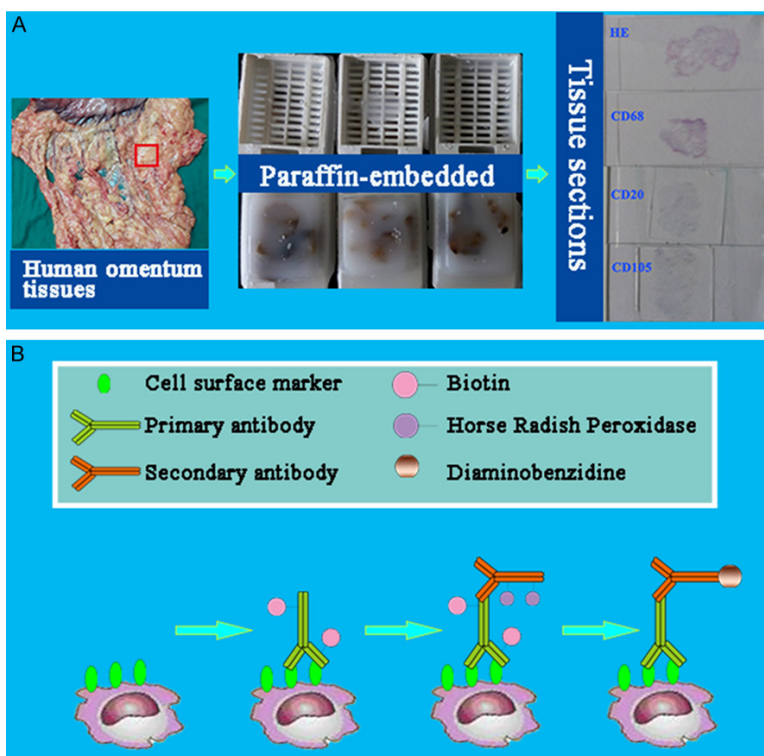
Figure 1. The design and major technical procedures of this study. A. Preparation of tissue sections. B. CD68, CD3, CD20cy, Calretinin and CD105 were imaged based on immunohistochemical method.

ies used were listed in **Table 1**. After blocking endogenous peroxidase activity with 3% H_2O_2 for 10 min to prevent any nonspecific binding, 2% bovine serum albumin (BSA) was used to block the slides to decrease background intensity. Then the slides were first incubated with primary antibodies respectively for 2 h at 37°C, then rinsed and incubated with corresponding secondary antibodies (dilution 1:300) for 30 min at 37°C. The reaction products were visualized with diaminobenzidine (DAB, DAKO, Denmark). As a negative control, the primary antibody was replaced with Tries-buffered saline on sections that were proven to be positive for Calretinin, CD-68, CD3, CD20cy and CD105 in preliminary experiments (**Figure 1B**).

Image acquisition

Slides were examined under Olympus BX51 microscope equipped with an Olympus DP72 camera (Olympus Optical Co., Ltd., Tokyo, Japan) at 10, 20 and 40× magnifications and the images were captured by DP72 camera.

Using pixel value to calculate the size of MS

We drew the outline of every MS on HE stained images under the guide of expert-pathologist (Jing-Ping Yuan). The morphological features of MS were shown as different shapes with corresponding proportions. A self-adaptive Otsu threshold method was adopted by digital image processing computer scientist Ai-Ping Qu [6] to convert the obtained images into binary imag-

in neutral formalin and processed by routine histological procedure, with the study protocol approved by ethnics committee of hospital. According to our previously established technical procedure [5], tissue sections (4 μm thickness) were treated by deparaffinizing, hydration, antigen retrieval, and washing in deionized water before proceeding to the following imaging studies (**Figure 1A**).

Immunohistochemistry

The immunohistochemistry (IHC) study was conducted to demonstrate mesothlial cells, macrophages, T lymphocytes, B lymphocytes and vascular endothelial cells. Primary antibod-
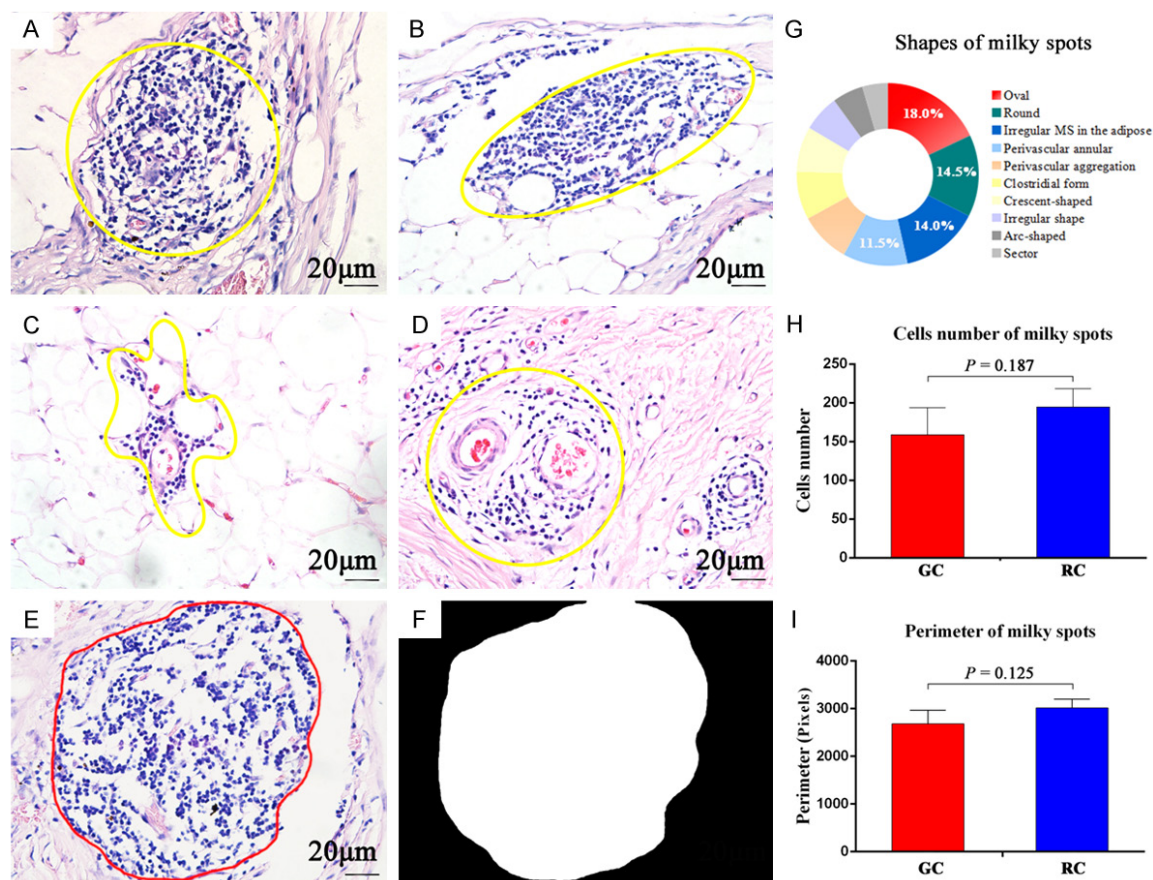
Figure 2. HE staining of milky spots. The yellow frame is used to show the gross morphology of MS: A. Round. B. Oval. C. Irregular form in adipose tissues. D. Perivascular annular. E→F. Using computer methods to convert HE images into binary images for calculation of MS perimeter. G. Proportions of MS shapes. H + I. Comparison of MS cells number and perimeter between GC and RC, respectively. (A→F: 400×, scale bar =20 μm.)

es. Then the perimeter of MS region could be output as pixel value spontaneously.

Cells counting methods

IHC stained results showed that outlines of T lymphocytes, B lymphocytes and mesothelial cells were clear enough to directly count cells number, while macrophages were in irregular shapes. In order to solve this problem, Imagepro Plus 6.0 software (IPP, Media Cybernetics, Inc., Washington, USA) [7] was operated to segment areas of interesting (AOI), that is brown macrophages of MS images as one color, and other cells of MS as another color. Then integrated optical density (IOD) of both color region could be obtained from the data output by IPP. The proportion of macrophages area was calculated subsequently by the equation that IOD Macrophages ×100%/IOD MS.

Microvessel density (MVD) was counted according to methods reported by Weidner et al. [8]. If separated with microvessels nearby or other connective tissues, every endothelial cell or endothelial cell clusters were treated as one microvessel. Formation of apparent lumen or exist of red blood cells was not judgment standard. In addition, blood vessels with lumen area more than 8 red blood cells or thick muscular layer were excluded.

Statistical analysis

Statistical analysis was performed with SPSS 21.0 software (SPSS Inc. Chicago, IL, USA). Results of cellular components number were expressed as median value with relevant range. Differences between MS from GC and RC were calculated by Mann-Whitney U test. Two sided $P<0.05$ was considered as statistically significant.
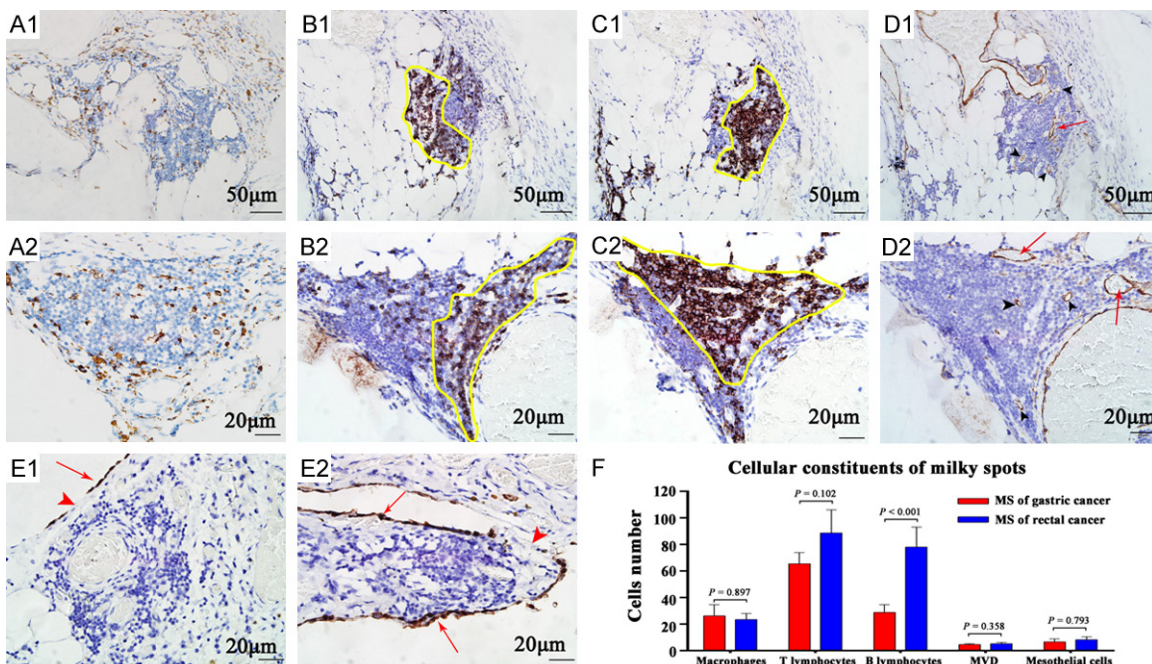
Figure 3. IHC staining of milky spots to analyze the cellular constituents. A. Macrophages are diffusely distributed within MS. B, C. Lymphocytes are located intensively in particular position. The location of T lymphocytes is roughly complementary with B lymphocytes, as shown by the yellow frame. D. Black arrow heads indicate microvessels in MS, while red arrows indicate vessels more than 8 red blood cells in diameter. E. Red arrows indicate mesothelial cells stained by Calretinin. Red arrow heads indicate the stomata of MS. F. Different cellular components of MS. (A1→D1: 200×, scale bar =50 μm; A2→E2: 400×, scale bar =20 μm.)

Table 2. Comprehensive parameters of milky spots

Parameters	Overall	Gastric cancer	Rectal cancer	P*
	Median (range)	Median (range)	Median (range)	
Total immune cells	141 (43~650)	130 (43~520)	145 (45~650)	0.187
Perimeter (pixels)	2752 (817~7753)	2545 (1104~4836)	2783 (817~7753)	0.125
Mesothelial cells	5 (0~51)	7 (0~17)	5 (0~51)	0.793
Macrophages (%)	12.4 (0.6~75.8)	14.7 (0.6~75.8)	10.7 (2.0~56.1)	0.897
T lymphocytes	65 (17~280)	57 (20~146)	68 (17~280)	0.102
B lymphocytes	40 (7~220)	21 (7~100)	66 (7~220)	<0.001
Micro-vessel density	4 (0~13)	4 (0~11)	5 (0~13)	0.358

*: Mann-Whitney U test.

Results

Results of HE staining

Morphological features of MS: One hundred MS images from GC slides and one hundred MS from RC were obtained by HE staining. After drawing outlines of every MS, we carefully classified various shapes as round (14.5%), oval (18.0%), irregular form in the adipose (14.0%), perivascular annular (11.5%), perivascular aggregation (9.0%), sector (4.5%), clostridial form (8.5%), arc-shaped along the omental edge (5.5%) and others (14.5%) (**Figure 2G**). The former four types were the main shapes (**Figure 2A-D**). It was fairly common to find MS within the edge of the omentum in RC images, while this phenomenon was not obvious for GC. However, all MS were rich in blood vessels and a cluster of immune cells.

Cells number and size of MS: The median MS cells number for GC was 130, ranging from 43 to 520. The corresponding data for RC was
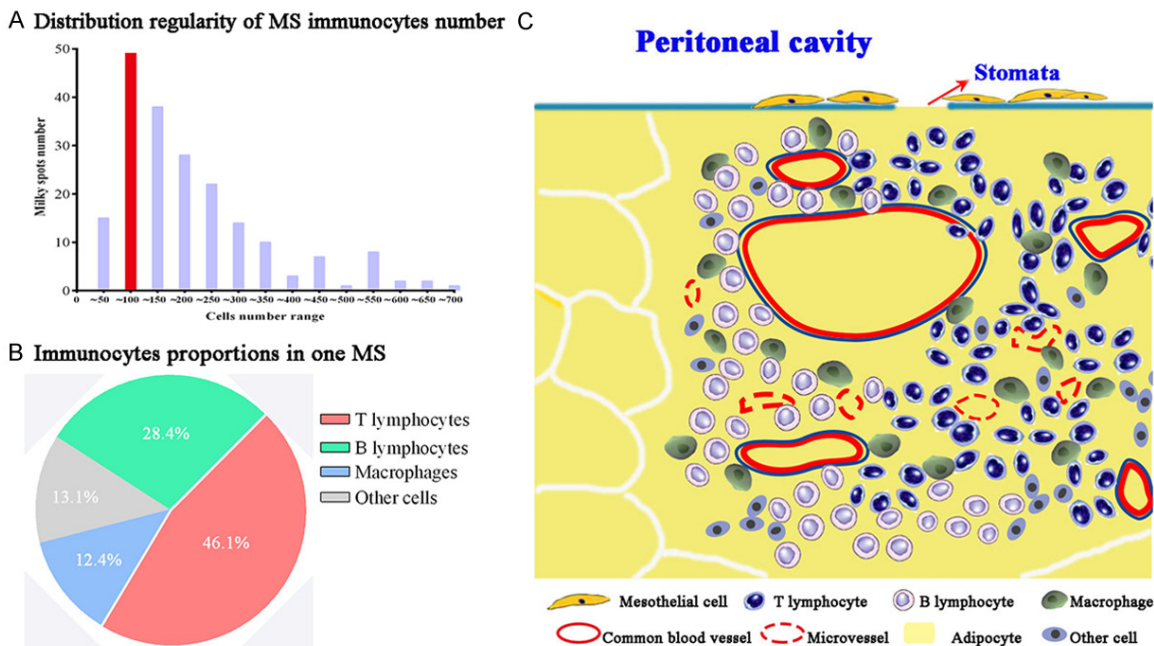
Figure 4. Morphological features of milky spots. A. Immunocytes number in one MS is mainly between 50 and 100. B. Immunocytes proportions of MS. C. The structure of MS: Leukocytes comprising macrophages, B cells, and T cells are arranged around the omental capillaries that lie directly beneath the discontinuous mesothelium with pores allowing for direct communication with the peritoneal cavity.

145, ranging from 45 to 650. There was no significant difference in MS cells number between GC and RC (*P*=0.187) (**Figure 2H**). The median MS perimeter for GC was 2545 pixels, ranging from 1104 to 4836 pixels. The corresponding data for RC was 2783 pixels, ranging from 817 to 7753 pixels. There was no significant difference in MS perimeters between GC and RC (*P*=0.125) (**Figure 2I**).

Results of IHC staining

Macrophages: Macrophages with different sizes and irregular shapes were diffusely distributed among other immune cells (**Figure 3A**). The percentage composition of macrophages varies considerably by the output data of IPP software. In GC MS, the median macrophages percentage was 14.7%, ranging from 0.6% to 75.8%. The corresponding data of RC was 10.7%, ranging from 2.0% to 56.1%, with no significant difference from GC (P=0.897).

T lymphocytes: T lymphocytes accumulated to form cell mass located in particular position in MS (**Figure 3B**). The median T lymphocytes number of GC MS was 57, ranging from 20 to 146. The data of RC was 68, ranging from 17 to

280. There was no significant difference in MS T lymphocyte number between GC and RC (P=0.102).

B lymphocytes: B lymphocytes also formed accumulations located in particular position roughly complementary with T lymphocytes in MS (**Figure 3C**). The median B lymphocytes number of GC MS was 21, ranging from 7 to 100. The data of RC was 66, ranging from 7 to 220. B lymphocytes number of GC MS was significantly higher than RC MS (P<0.001).

Vascular endothelial cells: Micro-vessels existed mainly in the internal layer of MS (**Figure 3D**). The median MVD of GC MS was 4, ranging from 0 to 11. The data of RC was 5, ranging from 0 to 13. There was no significant difference in MS MVD between GC and RC (P=0.358).

Mesothelial cells: The surface layer of MS was covered by mesothelial cells (MC) atop the aggregates of immune cells and blood vessels. The number of MC was approximately 3.6% of that of immune cells. MC was loosely arranged. Intercellular gaps and pores (stomata) are frequently found, and these openings expose underlying connective tissue matrix of MS

(**Figure 3E**) and gain access into the abdominal cavity. In addition, there are also accumulated MC presenting double layer in few MS (**Figure 3J**). The median MC number of GC MS was 7, ranging from 0 to 17. The data of RC was 5, ranging from 0 to 51. There was no significant difference in MS mesothelial cells number between GC and RC (P=0.793).

General parameters: The above results of every parameter were summarized in **Table 2**. We found cells number of MS in HE images was mostly between 50 and 100, accounting for 24.5% (49/200) of the total studied MS. Based on total immune cells number obtained from HE images, results of cellular components of IHC images showed that the proportion of T lymphocytes, B lymphocytes, macrophages and other immune cells was 46.1%, 28.4%, 12.4% and 13.1%, respectively. Based on these information of MS morphology and cellular components (**Figures 3F**, **4A** and **4B**), we designed an illustrative diagram of MS structure (**Figure 4C**).

Discussion

Induced by synergistic effect of tumor cells and microenvironment [9-11], activating invasion and metastasis is one of the six biological capabilities acquired during the multistep development of human tumors [12]. Peritoneal metastasis is a frequent cause of death from GC and RC, with the great omentum as a predominant metastatic site. It is mainly because of the specific primary immune tissues called milky spots (MS), which are interspersed within the omental environment [13]. In the light of seed-soil theory, peritoneal cancer cells dislodged from the primary tumor become seeds maintaining the ability of invasion and metastasis, and preferentially attach, subsequently survive and grow within MS [14]. The intimate and dynamic interactions between cancer cells and cellular constituents of MS are largely unknown.

Mesothelial cells in the surface layer of MS constitute the first line of defense against tumor cells. The omentum, like the rest of the peritoneum, is covered by a layer of mesothelial cells [15]. These mesothelial cells can be injured by external tumor cells and internal macrophages of MS [16], then probably undergo transformation into myofibroblasts in response to TGF-β1 [17, 18], thus creating a favorable microenvi-

ronment for peritoneal metastasis. In a word, the mesothelial cells are strong candidates for the preferential attachment of tumor cells on MS [13].

Immune cells constitute the main body part of MS. In our study, T lymphocytes form 46.1%, B lymphocytes 28.4%, and macrophages 12.4% of the immune cell population. Our quantification results differ from those described by Krist et al [19], in 1995. They reported a higher percentage of macrophages (67.9%±9.4, mean ± standard deviation). These differences can be explained by the following facts that a much higher number of MS are counted, more specific monoclonal antibodies are applied in our study, and MS is influenced by metastatic tumor cells to some extent. Other than cells proportion, positional relation of immune aggregates is analyzed by IHC technique as well. Lymphocytes tend to form accumulations located in particular position in MS, and T lymphocytes are roughly complementary with B lymphocytes. This phenomenon may represent or facilitate regional enhanced immunization for anti-tumor effect in early stages of metastasis. On the contrary, macrophages distribute diffusely in MS and along their border with surrounding tissues. In general, there are two forms of macrophages, classically activated (M1) and alternatively activated (or polarized, M2) [20]. M2 macrophages are also tumor-associated macrophages (TAM). Roles of TAMs vary in distinct microenvironments. TAMs promote metastasis in stromal and perivascular areas and stimulate angiogenesis in hypoxic avascular and peri-necrotic areas [21, 22]. We need further study of macrophages phenotype to distinguish whether TAMs have site-specific locations in MS, thus ensuring the correlation between the structure and functions of MS.

Finally, the most important requirement for survival and growth of metastatic tumor cells is a high density of vascular system within the target tissues [23]. Metastatic tumor cells have been found to migrate toward the closest microvessel and there start dividing [24]. Only in this way, these aggressive cells will gain a survival advantage for subsequent growth into metastatic foci. Based on our results of CD105 immunostaining, microvessels are mainly located in the internal layer of MS. As a proliferation-associated antigen, CD105 is located predomi-

nately on vascular endothelial cells undergoing active angiogenesis [25, 26]. Therefore, angiogenesis can be detected in MS once influenced by metastatic tumor cells. It also explains why MS is suitable for tumor survival and growth.

Except for changes of cellular components, the general morphology of MS is also influenced by metastatic tumor cells. Gerber et al. [27] have proved immune cell clusters in mice omentum are disrupted gradually after intraperitoneally injected with tumor cells. Once infiltrated with metastatic tumor cells, MS initially perform anti-tumor effect. After the apoptosis of mature cancer cells, remaining cancer stem cells [28, 29] maintain the ability to proliferate and differentiate by releasing varieties of chemokines, inducing angiogenesis and so on. MS region is replaced by proliferating cancer cells gradually after inherent cellular components withering away. In our study, round and oval MS are two main morphology with the most immune cells from HE images. Other MS are either in irregular shape or with fewer immune cells. Thus, we can propose that round and oval shapes represent the early stages of complete MS. In conclusion, the reduction of the number of MS in early stages is a sign indicating the progression of peritoneal metastasis.

Conclusion

MS are hotbeds for invasion and metastasis of intraperitoneal tumor cells. Quantitative analysis on different parameters of MS can be conducted separately by IHC technique to obtain preliminary morphological characteristics, cellular constituents of MS. As preferential sites for metastasis of GC and RC, MS deserve to be studied furthermore. The proportion and positional relation of cellular constituents in MS become structural basis for development and progression of the peritoneal metastasis.

Acknowledgements

Disclosure of conflict of interest

None.

Address correspondence to: Dr. Yan Li, Department of Oncology, Zhongnan Hospital of Wuhan University, Hubei Key Laboratory of Tumor Biological Behaviors and Hubei Cancer Clinical Study Center, 169 Donghu Road, Wuchang District, Wuhan 430071, China. Tel: +86-27-67812690; E-mail: liyansd2@163.com

References

[1] Glockzin G and Piso P. Current status and future directions in gastric cancer with peritoneal dissemination. Surg Oncol Clin N Am 2012; 21: 625-633.

[2] Mahteme H, Hansson J, Berglund A, Påhlman L, Glimelius B, Nygren P and Graf W. Improved survival in patients with peritoneal metastases from colorectal cancer: a preliminary study. Br J Cancer 2004; 90: 403-407.

[3] Lengyel E. Ovarian cancer development and metastasis. Am J Pathol 2010; 177: 1053-1064.

[4] Hagiwara A, Takahashi T, Sawai K, Taniguchi H, Shimotsuma M, Okano S, Sakakura C, Tsujimoto H, Osaki K, Sasaki S and Shirasu M. Milky spots as the implantation site for malignant cells in peritoneal dissemination in mice. Cancer Res 1993; 53: 687-692.

[5] Chen C, Peng J, Xia HS, Yang GF, Wu QS, Chen LD, Zeng LB, Zhang ZL, Pang DW and Li Y. Quantum dots-based immunofluorescence technology for the quantitative determination of HER2 expression in breast cancer. Biomaterials 2009; 30: 2912-2918.

[6] Wang LW, Qu AP, Yuan JP, Chen C, Sun SR, Hu MB, Liu J and Li Y. Computer-based image studies on tumor nests mathematical features of breast cancer and their clinical prognostic value. PLoS One 2013; 8: e82314.

[7] Gu J, Liang Y, Qiao L, Li X, Li X, Lu Y and Zheng Q. Expression analysis of URI/RMP gene in endometrioid adenocarcinoma by tissue microarray immunohistochemistry. Int J Clin Exp Pathol 2013; 6: 2396-2403.

[8] Weidner N, Folkman J, Pozza F, Bevilacqua P, Allred EN, Moore DH, Meli S and Gasparini G. Tumor angiogenesis: a new significant and independent prognostic indicator in early-stage breast carcinoma. J Natl Cancer Inst 1992; 84: 1875-1887.

[9] Wu SD, Ma YS, Fang Y, Liu LL, Fu D and Shen XZ. Role of the microenvironment in hepatocellular carcinoma development and progression. Cancer Treat Rev 2012; 38: 218-225.

[10] Peng CW, Tian Q, Yang GF, Fang M, Zhang ZL, Peng J, Li Y and Pang DW. Quantum-dots based simultaneous detection of multiple biomarkers of tumor stromal features to predict clinical outcomes in gastric cancer. Biomaterials 2012; 33: 5742-5752.

[11] Fang M, Yuan JP, Peng CW, Pang DW and Li Y. Quantum dots-based in situ molecular imaging of dynamic changes of collagen IV during cancer invasion. Biomaterials 2013; 34: 8708-8717.

[12] Hanahan D and Weinberg RA. Hallmarks of cancer: the next generation. Cell 2011; 144: 646-674.

[13] Sorensen EW, Gerber SA, Sedlacek AL, Rybalko VY, Chan WM and Lord EM. Omental immune aggregates and tumor metastasis within the peritoneal cavity. Immunol Res 2009; 45: 185-194.

[14] Jayne D. Molecular biology of peritoneal carcinomatosis. Cancer Treat Res 2007; 134: 21-33.

[15] Beelen RH. The greater omentum: physiology and immunological concepts. Neth J Sur 1991; 43: 145-149.

[16] Liu XY, Miao ZF, Zhao TT, Wang ZN, Xu YY, Gao J, Wu JH, You Y, Xu H and Xu HM. Milky spot macrophages remodeled by gastric cancer cells promote peritoneal mesothelial cell injury. Biochem Biophys Res Commun 2013; 439: 378-383.

[17] Lv ZD, Na D, Ma XY, Zhao C, Zhao WJ and Xu HM. Human peritoneal mesothelial cell transformation into myofibroblasts in response to TGF-β1 in vitro. Int J Mol Med 2011; 27: 187-193.

[18] Standiford TJ, Kuick R, Bhan U, Chen J, Newstead M and Keshamouni VG. TGF-β-induced IRAK-M expression in tumor-associated macrophages regulates lung tumor growth. Oncogene 2011; 30: 2475-2484.

[19] Krist LF, Eestermans IL, Steenbergen JJ, Hoefsmit EC, Cuesta MA, Meyer S and Beelen RH. Cellular composition of milky spots in the human greater omentum: an immunochemical and ultrastructural study. Anat Rec 1995; 241: 163-174.

[20] Martinez FO, Sica A, Mantovani A and Locati M. Macrophage activation and polarization. Front Biosci 2008; 13: 453-461.

[21] Lewis CE and Pollard JW. Distinct role of macrophages in different tumor microenvironments. Cancer Res 2006; 66: 605-612.

[22] Sica A. Role of tumour-associated macrophages in cancer-related inflammation. Exp Oncol 2010; 32: 153-158.

[23] Folkman J. Role of angiogenesis in tumor growth and metastasis. Semin Oncol 2002; 29: 15-18.

[24] Li CY, Shan S, Huang Q, Braun RD, Lanzen J, Hu K, Lin P and Dewhirst MW. Initial stages of tumor cell-induced angiogenesis: evaluation via skin window chambers in rodent models. J Natl Cancer Inst 2000; 92: 143-147.

[25] Fonsatti E and Maio M. Highlights on endoglin (CD105): from basic findings towards clinical applications in human cancer. J Transl Med 2004; 2: 18.

[26] Sánchez-Elsner T, Botella LM, Velasco B, Langa C and Bernabéu C. Endoglin expression is regulated by transcriptional cooperation between the hypoxia and transforming growth factor-beta pathways. J Biol Chem 2002; 277: 43799-43808.

[27] Gerber SA, Rybalko VY, Bigelow CE, Lugade AA, Foster TH, Frelinger JG and Lord EM. Preferential attachment of peritoneal tumor metastases to omental immune aggregates and possible role of a unique vascular microenvironment in metastatic survival and growth. Am J Pathol 2006; 169: 1739-1752.

[28] Cao L, Hu X and Zhang Y. Omental milky spots-highly efficient "natural filter" for screening gastric cancer stem cells. Med Hypotheses 2009; 73: 1017-1018.

[29] Xu G, Shen J, Ou Yang X, Sasahara M and Su X. Cancer stem cells: the 'heartbeat' of gastric cancer. J Gastroenterol 2013; 48: 781-797.